Design and Analysis of a Bidirectional Hybrid DC Circuit Breaker using AC Relays with Long Life Time

Ken King Man Siu, *Member, IEEE*, Carl Ngai Man Ho, *Senior Member, IEEE*, and Dong Li, *Student Member, IEEE*

***Abstract*- This paper presented a new hybrid circuit breaker solution for using in dc microgrids. The proposed solution can offer a high-reliability protection feature for the dc microgrid with low conduction loss, bidirectional current flow, and galvanic isolation function. In the design, it is combined with a group of mechanical switches and semiconductors, where the mechanical switches handle the current conduction during normal operation and the semiconductors handle the breaker response during transient operation. The design fully utilizes the advantage of both types of switches and maximizes the performance and life time of the system. Throughout the design, it maintains only one mechanical switch in series with each power line, thereby the high conductivity of the circuit breaker is maintained. At the same time, through the hybrid design, the electrical stress applied to the mechanical switch is eliminated. Thus, an effective and high-reliability solution is provided for the design of dc circuit breakers. The operation principle is explained in details and the design guideline is provided. A 150/380 V and 15 A circuit breaker is successfully implemented and the performance is experimentally verified which shows good agreement with the theoretical findings.**

Index Terms- dc circuit breaker, microgrid relay, semiconductor application

I. INTRODUCTION

The development of Smart Grid brings a technological revolution from the traditional centralized ac power network. In terms of technological development, the applications of renewable energy and battery energy storage elements have become more mature, and more and more appliances are changed to dc power. Therefore, the development of dc microgrids (MG) becomes the trend in future energy systems. It has already been applied in certain applications, such as marine smart ships, [1], [2], and dc residential grid networks, [3] - [5], and more applications will be developed in the coming future. The system architectures and the system control algorithms are two main research areas to develop dc MG technology. Apart from that, the system protection is another key concern in dc MG, as it is related to the safety and stability of the whole system. Especially in the application of low-voltage (LV) public power grids, for any power generation system and solar power system fed in parallel to the grid, automatic disconnection equipment must be installed, [6] – [8]. Its main purpose is to prevent any unintentional current from feeding into the sub-grid or independent grid during the system shutdown. Thus, regarding the safety concern, in such applications, protection circuits with high reliability and double line physical isolation characteristics are always required.

In the past few years, due to the increasing popularity of dc MG, various hybrid protection solutions, [9]- [22], have recently been proposed to provide high-quality protection features and to overcome the reliability issues of the traditional mechanical breaker solutions. The concept of hybrid solution firstly appears in the ac grid system. In [9], a typical ac hybrid switching scheme is proposed in which a thyristor is in parallel with the mechanical switch to interrupt the short circuit current. As shown in Fig. 1 (a), similar to [9], a typical hybrid dc circuit breaker solution is presented in [10], in which a fast mechanical switch and integrated gate control thyristor (IGCT) sets are connected in parallel. The IGCT is applied to handle the transient operation during the turn-off moments and to effectively improve the reliability of the circuit. However, the galvanic isolation function of the relay is disabled. An optional design is presented in [11] which is in a parallel combination of similar semiconductor devices to generate with the same functionality. In [12], a hybrid circuit breaker with a forced commutation circuit is presented and its circuit diagram is given in Fig. 1 (b). By the circuit operation, it can commutate the current to the parallel path before the mechanical circuit breaker is opened. Therefore, the total system shutdown time can be reduced, which is stayed between mechanical and solid-state solutions. However, the circuit capacitor is required to pre-charge and the galvanic isolation function of the relay is disabled. Another type of hybrid circuit breaker is proposed in [13], and its circuit configuration is shown in Fig. 1 (c). In the design, the main conduction path is formed by a mechanical switch and a pair of bidirectional semiconductor switches, and the alternative conduction path is formed by another pair of bidirectional semiconductor switches. Two sets of semiconductors pair are with different functions in the circuit, where the main path one is acted as a commutation switch and the alternative path is acted as the main breaker. Accordingly, compared with [10], a relatively faster short-circuit response can be obtained. However, due to the presence of two sets of semiconductor pairs in the circuit design, a higher system conduction loss is resultant and no galvanic isolation function is offered. Under the same functionality as [13], various solutions are given in [14] - [17], which are with different semiconductor combinations.

Ken K.M. Siu (Corresponding author), Carl N.M. Ho and Dong Li, are with the RIGA Lab, the Department of Electrical & Computer Engineering, University of Manitoba, R3T5V6, Winnipeg, MB, Canada (E-mail: siukm3@myumanitoba.ca).

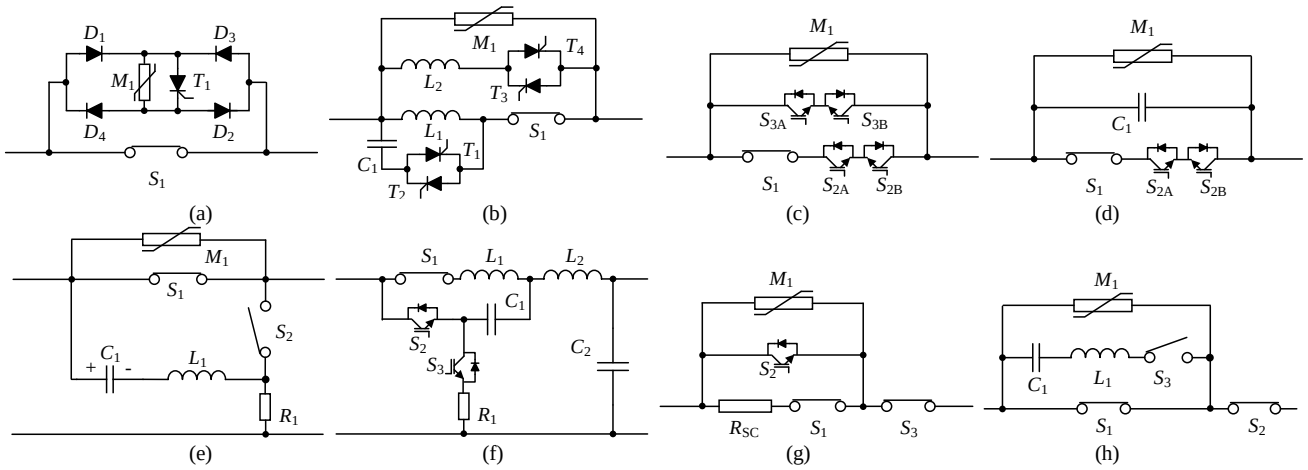

Fig. 1 Prior-arts of dc circuit breaker.

TABLE I SUMMARY OF NUMBER OF SEMICONDUCTOR DEVICES AND MECHANICAL COMPONENTS INVOLVED IN THE TOPOLOGIES

Topology	Main Conduction Path			Auxiliary Path			Breaking Action in S_1	Major Function			
	Switch		Passive Device	Switch		Passive Device		Bidirectional	Durability	Galvanic Isolation	Possibility of Overvoltage
	Type	Total Cond.		Type	Total Cond.						
Fig. 1a	1 Mech.	1	0	5 Semi.	3	0	LV Turn-off	Yes	High	No	High
Fig. 1b	1 Mech.	1	1	4 Semi.	1	2	ZCS	Yes	High	No	High
Fig. 1c	1 Mech. + 2 Semi.	3	0	2 Semi.	2	0	ZCS	Yes	High	No	High
Fig. 1d	1 Mech. + 2 Semi.	3	0	0	0	1	ZCS	Yes	High	No	High
Fig. 1e	1 Mech.	1	0	1 Power Switch	1	3	ZCS	No	High	No	Middle
Fig. 1f	1 Mech.	1	2	1 Semi.	2	1	ZCS	No	High	No	Low
Fig. 1g	2 Mech.	2	1	1 Semi.	1	0	LC Turn-off	No	High	Yes	High
Fig. 1h	2 Mech.	2	0	1 Power Switch	1	2	ZCS	No	High	Yes	Middle
Fig. 2 (proposed)	1 Mech.	1	0	1 Mech. + 2 Semi.	2	0	LV Turn-off	Yes	High	Yes	Low

In addition, in [18], an alternative solution of [13] is proposed in which the semiconductor pair in the auxiliary conduction path is replaced by a capacitor, as shown in Fig. 1 (d). Therefore, the design is simplified and the number of components is reduced. However, compared to [13], the component stress in the design becomes higher and additional discharging may require the fast reclosing application. In [19] and [20], two different types of zero current switching (ZCS) hybrid circuit breaker solutions are presented, as shown in Fig. 1 (e) and (f) respectively. Both are using a pre-charged capacitor to create resonant characteristics in the system during the turn-off transient and guide the current through the system to ensure ZCS. In [19], the reactor is connecting in series with the pre-charge to control resonant peak during breaking action and handle the capacitor charging action during the normal operation. The switch in the alternative conduction path can implement by a solid-state switch or other high power switching devices. In [20], the reactor is connecting in series with the mechanical switch in the main conduction path to slow down the current flow and two semiconductor switches are applied to control the interruption process. Both [19] and [20] have a highly efficient design, however, these ZCS solutions cannot provide galvanic isolation and bidirectional functions. To address the isolation feature, some isolated type hybrid solutions have been developed, [21] - [23]. In [21], an isolated hybrid solution is presented as shown in Fig. 1 (g). In the design, two mechanical switches are involved in the main current path. One is used as the main circuit switch, which will trigger immediately when a turn-off signal is provided, and the other is used to generate the isolation function. Since the number of mechanical switches is twice that of traditional mechanical solutions, it will cause the conduction loss in the system to double. In [22], a ZCS type isolated hybrid circuit breaker is presented as shown in Fig. 1 (h). The switch in the alternative conduction path can be a solid-state switch or other high power switching devices, such as spark gaps. However, similar to [21], the overall conduction loss on the positive line remains twice that of the traditional single mechanical solution. Meanwhile, with a similar feature as [22], another series *LC* type isolated hybrid circuit breaker is presented in [23]. Overall, a summary is given in TABLE I. In most cases, they have a higher probability of causing overvoltage on the switching devices.

Therefore, metal oxide varistor (MOV) is always required. In addition, among those reviewed hybrid designs, they are either not supporting the galvanic isolation feature or having high conduction loss in the design but cannot achieve both at the same time.

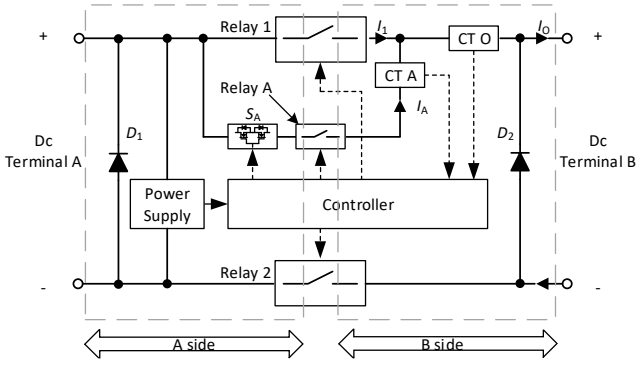

Fig. 2 The proposed dc circuit breaker.

An alternative high-reliability hybrid circuit breaker solution, as shown in Fig. 2, is proposed in this paper to achieve both galvanic isolation and high-efficiency features. It is aimed at LV dc MG applications and provides with low conduction loss, low device electrical stress, bidirectional current flow, and double line physical isolation feature on the entire system. In the design, each main power path is handled by a single mechanical relay to produce a low resistance connection path and a physical isolation during the turn-on and turn-off periods respectively. A mixed switch auxiliary path is given in the hybrid solution to separately handle the transient process. Thus, a smooth current exchange between the main conduction path and the auxiliary conduction path is realized and the electrical stress in the mechanical relay is minimized. Therefore, the durability of the mechanical relay is enhanced and it provides the possibility of using an ac relay in a dc circuit. Meanwhile, by combining the characteristics of protection diodes and auxiliary path, the proposed circuit has the surge current capability and the possibility of overvoltage is highly reduced. Therefore the overall solution is with high reliability and high efficiency. The operation principles of the presented solution and the design guideline are given in this paper. Targeting to LV dc MGs, a 150/380 V and 15 A experimental prototype has been implemented to verify the operation of the proposed circuit. The experimental results and detailed findings were consistent with the theoretical analysis.

II. Principle of Operation

A. Circuit Structure

The proposed solution consists of two main conduction paths and an auxiliary conduction path, where the main paths are composed of two main power relays, Relay 1 and 2, and the auxiliary path is formed by a pair of semiconductor devices, S_A, and a series auxiliary relay, Relay A. Meanwhile, two identical diodes, D_1 and D_2, are included in each terminal ends for the protection purposes. Two sets of current sensors, CT_A and CT_O, are applied to measure the power line current and the auxiliary line current, as i_O and i_A separately. The details of the configuration are shown in Fig. 2.

Among those three mechanical relays, two of them are used to provide isolation on the main conduction path and the third one provides isolation in the auxiliary conduction path. As a result, when a fault appears, both sides of the breaker circuit system can be physically isolated and a safe system environment can be guaranteed in the targeting MG application. Relays 1 and 2 are the two main relays in the circuit, which are used to establish the connection path between two system ends for the normal operation. Relay A is the auxiliary relay in the circuit, which is used to establish the connection path for the semiconductor pair and acts as the major conduction channel during the transient process. Both Relay 2 and Relay A operate at ZCS, and Relay 1 always switches with a parallel conduction channel. Therefore, component stress faced at the switching transients can be significantly reduced.

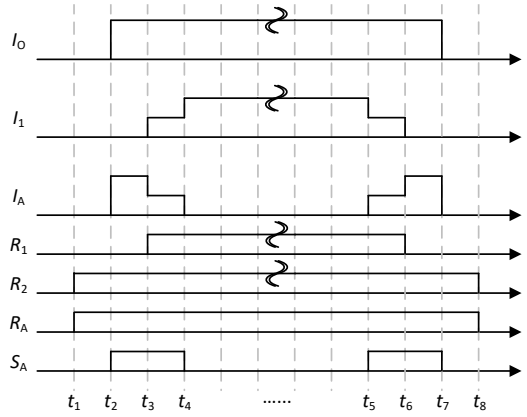

Fig. 3 The operation sequence of the proposed dc circuit breaker.

The pair of semiconductor devices only function actively during the turn-on and turn-off transient period, and acts as a main breaker of the whole system. The semiconductors are used to compensate for the energy during breaking action instead of using mechanical relays. As a result, the durability of the mechanical breaker system is enhanced and a fast breaker action can be achieved in any current or loading conditions. Thus, the proposed solution is with high system reliability. It can be realized by connecting two MOSFETs back-to-back in series connection or other bidirectional blocking switch configurations.

The pair of diodes may only function actively during the off transient and act as protective devices in the circuit to avoid any overvoltage conditions caused by the induced energy. Therefore, different from other hybrid solutions, [10], [12], [18], in the proposed solution, the semiconductor pairs will not reach the overvoltage value. The resultant electrical stress in the components is less than others and a parallel MOV is not required in the design. In order to realize the bidirectional protection function in the designed system, it is necessary to place an identical diode on each terminal.

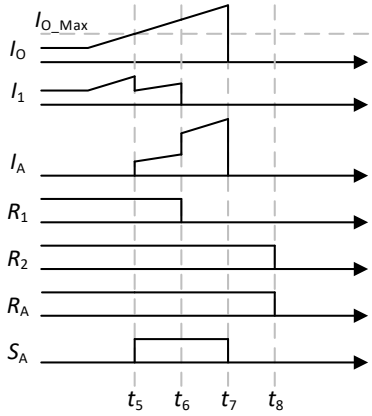

Fig. 4 Operation sequence during fault detection.

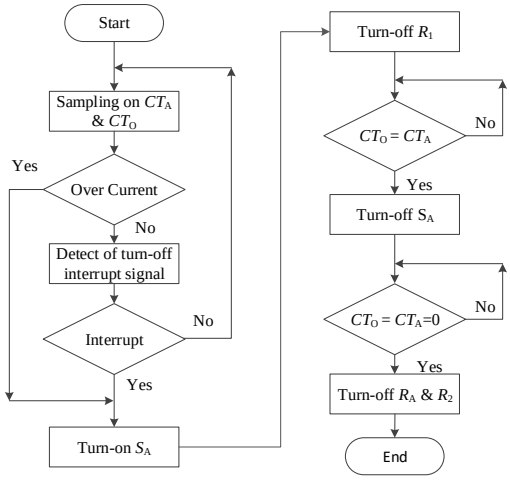

Fig. 5 Program flow in turn-off sequence.

In order to achieve a smooth current transient in the mechanical relays, a specific operation sequence is required. The accurate fault detection and a correct switching pattern are produced from the sensing information. According to the operating situations, the dc breaker will operate in different scenarios. A detailed operational sequence at the normal situations is given in Fig. 3 and Fig. 4, respectively. Also, a program flow of the turn-off sequence is given in Fig. 5.

B. Operation Sequence at Turn-on Situation

Stage 1 [t= t_1] - After the start-up signal is given, the circuit begins to operate. Turn-on signals are given to R_2 and R_A. During this time, R_2 becomes ON and provides a return path for current. At the same time, the physical isolation of the auxiliary path is removed. R_A becomes conduction and establishes a path to connect semiconductor devices to both system terminals. At this period, the main conduction path is not yet established, so no current flows through the circuit. This stage accomplishes when R_2 and R_A are fully conducted.

Stage 2 [t= t_2] - A turn-on signal is given to S_A to release the bidirectional blocking from the semiconductor devices. During this time, S_A becomes ON and a connection path between both ends of the circuit is established as an auxiliary channel. The dc current starts to flow from one terminal to the other through the auxiliary path as I_A. This period ends after the semiconductor is fully ON.

Stage 3 [t= t_3] - A turn-on signal is given to R_1. During this time, R_1 becomes ON. Due to the presence of the auxiliary path, R_1 can switch under a relatively LV condition and within the ac relay specified dc switching voltage. The major connection path between both positive terminals is built up. Due to the lower resistance characteristic, the dc current will bypass the auxiliary path and start to flow through R_1 as I_1. The overall output current, I_O, remains the same at the last stage, however, I_A is reduced. This period will end after R_1 is fully ON at a certain time and a current reduction in I_A is detected.

Stage 4 [t= t_4] - A turn-off signal is given to S_A to disable the auxiliary conduction path. During this time, S_A becomes OFF and switches under a relatively LV condition. Afterward, the auxiliary channel is electrically disconnected from the main circuit. The dc current will only flow through the main relays, in which I_1 becomes the same as I_O. This period ends when I_1 becomes zero. And the system turn-on transient sequence is finished and only two main relays are remaining ON.

C. Operation Sequence at Turn-off Situation

Stage 5 [t= t_5] - After a disconnection signal is given from the general shutdown operation or the fault detection, the circuit turn-off operation sequence begins. A turn-on signal is given to S_A to set up an auxiliary conduction path for the power flow and the current conduction behavior will be the same as in Stage 3. This period will end after the semiconductor is fully ON and a current reduction in I_1 is detected.

Stage 6 [t= t_6] - A turn-off signal is given to R_1. During this time, R_1 becomes OFF. Due to the presence of the auxiliary path, R_1 can switch under a relatively LV condition and within the ac relay specified dc switching voltage. The main conduction path in the positive terminal is disconnected, thus, I_1 is forced to zero. The circuit remains conducting and the situation is the same as in Stage 2. This period ends after R_1 is fully OFF and the current value of I_A is exactly equal to I_1.

Stage 7 [t= t_7] - A turn-off signal is given to S_A to disable the auxiliary conduction path. During this time, S_A becomes OFF and it acts as the main breaker during this period. All energy among the breaking action will be dissipated through the semiconductor devices. Therefore, the selection of the semiconductor is very significant in the design. This period ends when I_1 becomes zero and the bidirectional blocking feature is reformulated. No more current is flowing through the breaker circuit.

Stage 8 [t= t_8] - A turn-off signal is given to both R_A and R_2. During this time, both relays become OFF and switch under ZCS operation. At the turn-off transient, no electrical stress is applied to the device. Afterward, both of the

auxiliary path and the current return path are physically disconnected from the main circuit. As a result, through the dc circuit breaker, both sides of the systems are fully isolated from each other. This can guarantee to have a safe environment for workers during grid or device repairing. The circuit remains OFF until a reconnection signal is given.

D. Arc Characteristic During Breaking

The major difference between the traditional mechanical solution and the proposed hybrid solution is on the arc handling. A set of electric performance comparisons is given in Fig. 6 (a) and (b) to demonstrates the difference between both solutions.

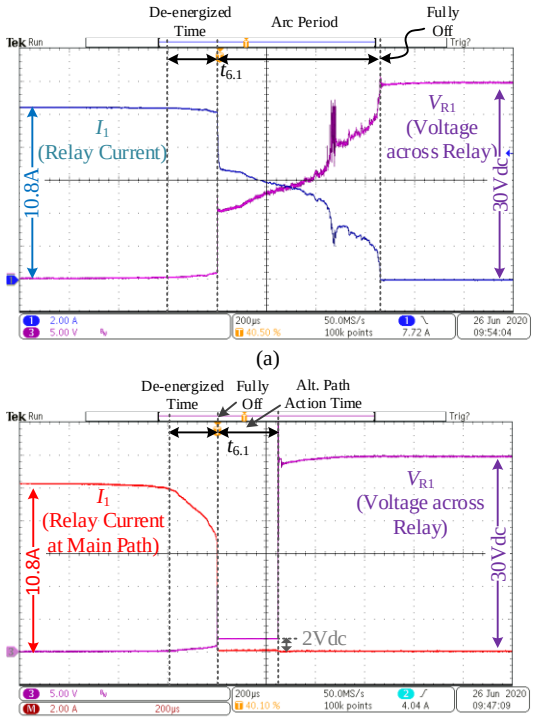

Fig. 6 Breaking waveforms of (a) traditional mechanical solution and (b) proposed breaker solution.

TABLE II PERFORMANCE SUMMARY A 30 VDC AND 10.8 A SYSTEM

Solution	Energy Dissipation	Duration
Mechanical Fig.6 (a)	45.82 mJ	660 µs
Proposed Fig.6 (b)	167.3 µJ	140 ns

In the traditional mechanical solution, as shown in Fig. 6 (a), when the opening signal is provided to the circuit breaker, the coil energy will start to be eliminated which causes the contacting plane to be separated and restored to its original position. Afterward, the contacting plane will begin to separate, the contacting area will be reduced which leads to an increase in both contacting resistance and current density on the contacting plane at the same time. Thus, the pressure between the contacts decreases and the temperature on between increases. At $t_{6.1}$, the contact planes are separated. In the case of low pressure and high temperature, the air in between will be ionized, thereby creating a low-resistance path for the main current to pass through. That is the arc we can observe [25], [26]. The intensity and duration of the arc mainly depend on the voltage stress and current magnitude. The energy dissipated during the mechanical breaking action can also be estimated based on the total cross-sectional area in the electrical waveform. When the contact returns to its original position and has high resistance insulation, the circuit breaker will completely open again.

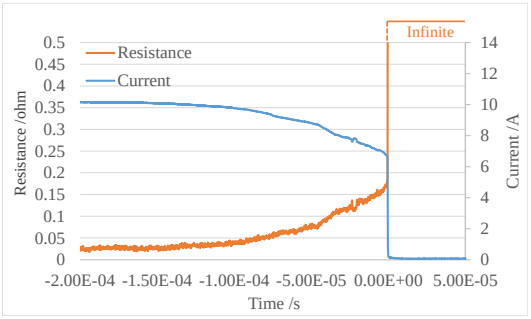

(a)

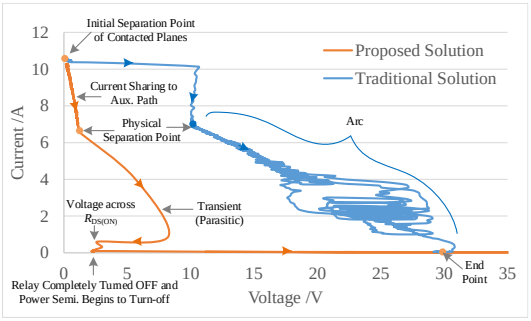

(b)

Fig. 7 Main relay performance diagram, (a) resistance change with time and (b) switching trajectories during stage 6.

In the proposed hybrid solution, the de-energized process is similar to the traditional solution. However, due to the existence of the auxiliary conduction path, when the contacting area begins to decrease, only the contacting resistance will increase, but the current density on the contacting plane will not be affected. It is also proofed in Fig. 6 (b), since the contacting resistance keeps increasing at the separation period, a significant current reduction is observed. At $t_{6.1}$, the contact planes begin to separate, the dc current will be immediately transferred from the main conduction path to the auxiliary conduction path and the transient process will be completed in a very short period of time under a relatively low voltage condition. Through Fig. 6 (b), it clearly demonstrates the benefit of the proposed method, in which the energy dissipation during the turn-off transient is reduced to µJ range and is 274 times lower than the traditional solution. A detailed summary table is given in TABLE II. In most cases, because the energy dissipated in the mechanical switches is limited in a small amount of value, the contacts will no longer rise to a high temperature value at the transient action and the ionization will not occur. In the meantime,

TABLE III SYSTEM PARAMETERS COMPARISON WITH COMMERCIAL PRODUCTS

Model	Hongfa -HFS33/D-200D10M	Crydom -84137850	TE Connectivity -AP10B245	Omron Electronics -G9EB-1	Proposed
Type	SolidState	SolidState	Mechanical Vacuum Relay	Mechanical with gas-filled	Hybrid
DC Voltage /V	200	200	270	250	380
DC Current /A	10	10	10	20	15
Max Surge /A (10ms)	40	60	N.A	N.A	80
Resistance / Ω	105m	210m	10m	30m	< 5m
Electrical Durability	> 100k	> 100k	7k	30k	> 100k
Dielectric Strength	N.A	N.A	2000 Vrms	2500 Vrms	1000 Vrms

according to Fig. 6, the corresponding resistivity over time and the switching trajectories at the turn-off transient are found and are given in Fig. 7(a) and (b), respectively. It clearly showed that no ionized low conduction path had resulted and the main relay was able to turn-off in a relative LV range. Thus, the possibility of arcing is highly reduced and a smoothly reopening is able to provide in each mechanical switching action. By having an appropriate circuit design, the energy dissipated in the mechanical switch can be limited to a specific value that does not cause ionization and arcing. Even in some unexpected situations, the energy is higher than expected, and the mechanical relay still has the ability to handle the arc at the specified power rated of the relay, and will not cause any system failure. A detailed switching diagram on the positive terminal is also given in Fig. 8 to explain the current flow during the turn-off transient.

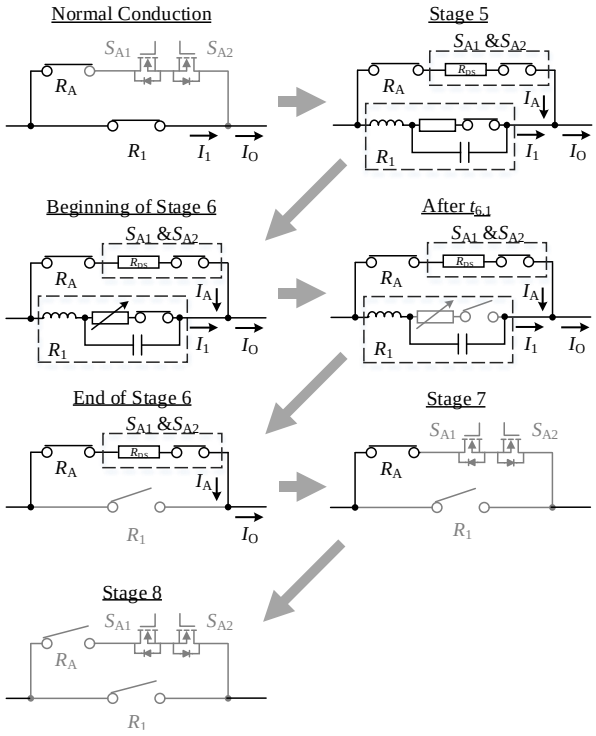

Fig. 8 Equivalent circuit on positive terminal during turn-off transient.

III. SELECTION OF COMPOMENTS

The proposed circuit is a hybrid dc breaker solution, which consists of both mechanical relays and semiconductor devices. In a traditional dc breaker solution, a single mechanical relay or a solid-state breaker is applied to act as both power line current conductors during the normal situation and circuit breaker during the transient situation.

Among the traditional breaker technologies, mechanical relay and solid-state relay are two of the commonly used devices. Some of the existing dc breakers on the markets are listed in TABLE III as reference. The key features are highlighted in the table. The mechanical relays are physical switches, which use the electromagnetic contact to control the circuit operation. They are with low conduction resistance and can provide high-level insulation on the device. However it is not able to handle the surge current and the durability is usually poor, around 10 k times. In contrast, the solid-state relays are most likely semiconductor-based. It provides fast response and low contacting arc. The drawback is the high conduction resistance and the absence of physical isolation. Hence, for solid-state relays, the overall system reliability is limited and the system efficiency is restricted.

Different from the single breaker solution, in the proposed solution, the major functions in the dc breaker circuit solution are separated clearly into two divisions, current conduction and circuit breaking. Each function is handled by a certain device, the advantage of both types of device can be fully utilized while their disadvantages are eliminated in the hybrid solution. In the design, mechanical relays are selected to handle the current conduction in the power line during the normal situation, and semiconductor switches are selected to handle the breaking action during the transient period. The target system parameter is highlighted in durability is TABLE III.

A. Selection of Mechanical Relays

In the traditional approach, during each switching action, an electrical arc will be generated between the two contacted planes. One of the examples is given in Fig. 9 (a), which is conducted under the on-site test. Under high voltage and high current on-off actions, the resulting high energy electrical arc

TABLE IV Selected components in the prototype

Device	Requirement			Selection	
	Conduction	Isolation	Switching	Model	Type
R_1	Power Line	Yes	Low Voltage	G2R-1A-E	AC Mechanical Relay
R_2	Power Line	Yes	ZCS	G2R-1A-E	AC Mechanical Relay
R_A	Auxiliary Path	Yes	ZCS	G2R-1A-E	AC Mechanical Relay
S_A	Auxiliary Path	No	None	IPW60R125C6	MOSFET

(a) (b)

Fig. 9 Experimental diagrams of mechanical relay (a) during electric arcs and (b) after repetitive switching action.

will heat the contacted plane and oxidize a small portion of the surface in each time. For the oxidized area will result in high resistive and influence the next performance. After a long term repetitive breaking action, the surface will be completely oxidized and the contactor may be bent, as shown in Fig. 9 (b). As a result, the relay will no longer function properly and result in failure.

In the proposed solution, mechanical relays are applied to handle the current conduction in the power line during the normal situation and to provide a physical isolation feature. Thus, when selecting, both voltage and current ratings are important parameters to be considered. The voltage rating of the relay is used to support the breakdown voltage of the ystem and the current rating of the relay is used to handle the current capability during the conduction period. Meanwhile, response time is another parameter in concern. In the proposed solution, it targets for low voltage public grid application. Thus, it is required that the selected relay has a response time of ms.

As discussed in Section II, different from the traditional approach, in the proposed solution, all the mechanical relays are switched under low energy dissipation condition. Therefore, in the proposed solution, the choice of relays becomes more extensive, the design can consider:

1) The use of ac relays in a dc relay circuit. All the relays are switched under either relatively LV or floating conditions,which means that the electrical stress applied to the components during the transient actions is at a relatively low value and can be limited within the ac relay specified dc switching voltage. The ac voltage rating of the relays is only used to guarantee that the circuit with enough voltage insulation for the system. Therefore, ac relays can be adopted into the selection on the mechanical relays instead of the bulky and expensive dc relays. For example, a 250Vac relay can apply to a dc circuit breaker design up to 353.6 Vdc. Therefore, it is especially suitable for LV dc MG.

2) Mechanical durability as relay durability instead of using electrical durability. The main power relay R_1 is always paralleled with a low resistance path during the switching transient. Thus, a smooth current transient is always guaranteed in R_1. The other two relays, R_A and R_2, are even better which are switched under zero current situation. All the relays are switched with low energy dissipation and the possibility of the electrical arc becomes relatively small. Accordingly, it provides an opportunity to extend the electrical durability of the applied mechanical relays to a value close to the mechanical durability defined in the datasheet and result in a longer lifetime in the entire solution compared to the traditional fully mechanical solution. The extension of life time will be more dependent on the maximum amount of energy dissipation in the mechanical relays.

Overall, in the target 150/380 Vdc and 15A dc breaker system, an ac relay, G2R-1A-E, is selected. It features with a 16A current capability, a maximum 380 Vac switching voltage, 100 k times in mechanical durability, 2 mΩ low resistance characteristic, and 7-9 ms mechanical action time. Thus, it fits for the target power ratings and helps to produce designs with high durability and high efficiency.

B. Selection of Semiconductors

In the design, semiconductor switches are applied to handle the transient switching action in the breaker circuit. A pair of semiconductor switches are required to apply at the same time to produce the bidirectional blocking characteristic. For discrete devices, they can be arranged into a back-to-back, drain-to-drain, or other bidirectional

configuration. In the selection, the voltage and current ratings of the semiconductors are determined by the operating voltage and the current capability of the system, respectively. In addition, inrush current capability is another parameter to consider in semiconductor selection. It is used to support the system response during faults and is defined by the maximum short circuit current and the worst-case energy information in the system.

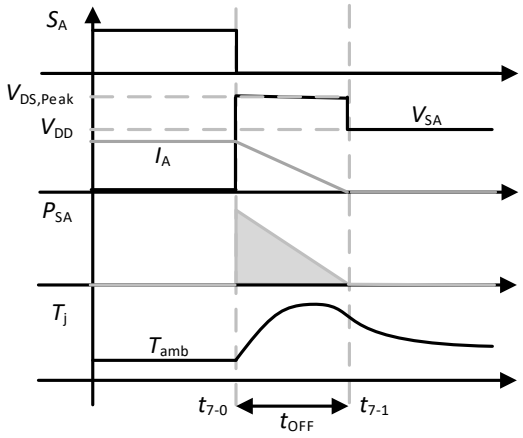

Fig. 10 MOSFET overvoltage performance at stage 7.

Among the switching sequences, the most critical breaking action appears in stage 7. At stage 4 and stage 5, S_A is switched ON and OFF under relatively low voltage conditions, respectively. However, at stage 7, due to the presence of parasitic inductance in the loop, high voltage stress will occur between the drain and source of the semiconductor under the turn-off transient. The detailed switching action of S_A during stage 7 is given in Fig. 10.

A pair of protection diodes has been applied to the system, generally, no overvoltage conditions will occur. However, for IGBTs or other semiconductor devices that without overvoltage capability, a parallel MOV is still recommended to avoid any excessive transient voltages. Differently, power MOSFET doesn't have this requirement. Inside a traditional MOSFET, there is a group of parasitic components inside the physical structure, such as parasitic resistance in P-well channel structure and a parasitic NPN bipolar transistor structure [27]. Normally, the parasitic NPN is effectively shorted. However, during the turn-off moment, a strong electric field is resultant inside the device which causes current flow proximity to the parasitic NPN transistor internally. Once the current flow causes sufficient voltage across on it, the parasitic bipolar transistor will become activated and will claim the device voltage at a value that is 1.2 to 1.3 times higher than the general breakdown voltage. Thus, power MOSFET can protect by the avalanche mode during the worst-case scenario and more suitable for the LV MG applications.

The worst-case energy is able to determine from the circuit relationship at stage 7. By applying Kirchhoff's voltage law to the main current loop, the detail characteristic of the overvoltage or the avalanche period can be determined. The circuit relationship at stage 7 is formed as,

$$V_{\mathrm{DD}} = V_{\mathrm{DS,Peak}} + L_{\mathrm{loop}} \cdot \frac{dI(t)}{dt} + R_{\mathrm{loop}} \cdot I(t), \quad (1)$$

where V_{DD} is dc voltage at the input side, $V_{DS,Peak}$ is overvoltage or the avalanche voltage applied to the semiconductor in stage 7, I is dc current flowing in the circuit, L_{loop} is loop inductance or parasitic inductance in the current path and R_{loop} is parasitic resistance at the current path.

By solving (1) with the start point and the endpoint circuit information, the corresponding turn-off time, t_{OFF}, is determined as,

$$t_{\mathrm{OFF}} = \frac{L_{\mathrm{loop}}}{R_{\mathrm{loop}}} \ln\left[1 + \frac{I_{\mathrm{peak}} \cdot R_{\mathrm{loop}}}{V_{\mathrm{DS,Peak}} - V_{\mathrm{DD}}}\right]. \quad (2)$$

During the turn-off period, the power dissipation in the MOSFET is approximating to a triangle waveform. According, the corresponding energy dissipation, E_{OFF}, is simplified to,

$$E_{\mathrm{OFF}} \cong \frac{1}{2} \cdot V_{\mathrm{DS,Peak}} \cdot I_{\mathrm{peak}} \cdot \frac{L_{\mathrm{loop}}}{R_{\mathrm{loop}}} \ln\left[1 + \frac{I_{\mathrm{peak}} \cdot R_{\mathrm{loop}}}{V_{\mathrm{DS,Peak}} - V_{\mathrm{DD}}}\right]. \quad (3)$$

With the use of (3), the maximum rating in the target system and a 2 μH parasitic loop inductance as the worst case assumption, a 0.2 mJ worst-case energy dissipation can be calculated.

According to the maximum rating of the target system, 150/380 Vdc and 15 A, the worst-case energy dissipation, 0.2 mJ, and a five-time short circuit capability, 75 A, in the target dc breaker system, a discrete TO247 power MOSFET, IPW60R125C6, is selection. It features with a 0.96 mJ for repetitive energy, around 89 A pulse current at 25℃, and with a 600 Vdc breakdown. A summary of the selected components is given in TABLE IV.

IV. Experimental Verifications

A 150/380 Vdc and 15 A test platform with a dc breaker prototype, as shown in Fig. 11, is built to verify the performance of the proposed dc circuit breaker and the target operating conditions defined in TABLE I. The prototype shows that the entire system is controlled by a single microcontroller and the protection feature comes from the accurate current detection by the Hall-effect sensors. Compared to the two relays traditional system, in the proposed solution, an extra relay and a pair of semiconductor switches were applied, in which the semiconductor pair were arranged in back-to-back connection. According to the given control strategy, the power consumption of the auxiliary circuit was kept within 3 W. At the standby mode, only 0.95 W was consumed. At the normal operation mode, 2.85 W was consumed, which is closed to the traditional approach.

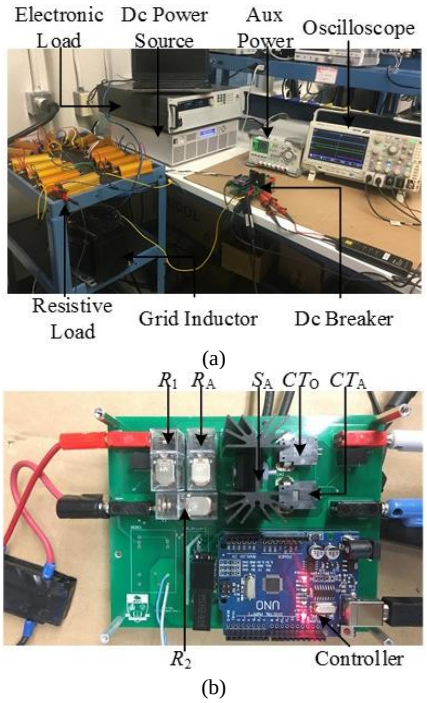

Fig. 11 Hardware diagrams of (a) test setup and (b) dc circuit breaker prototype.

In Fig. 12, it demonstrates a complete operating sequence of the proposed circuit during on and off conditions under a 10 Ω resistive load and 150Vdc input. The resultant operational sequence was the same as the one proposed in Section II. Each transient operation, it was able to divide into two parts, the electrical operation process, $T_{ON,SW}$ and $T_{OFF,SW}$, and the physical setting process, $T_{ON,SET}$ and $T_{OFF,SET}$. In both actions, their durations are also highly dependent on the response time of mechanical relays, which are about 7 to 9 ms. For example, in Fig. 12 (a), after the turn-on signal provides to R_1 at t_1, it takes 8 ms to settle, and then the semiconductors respond in another few hundred ns and complete the electrical operation process. A similar situation appeared in the physical setting process. Overall, the electrical transient action was able to complete in 8 ms, which fulfills with requirement protect feature in dc MGs of fault current interruption within 0.01 s [28], [29], and is compatible with other mechanical-based LVDC hybrid circuit breaker solutions and mechanical solutions in ms response time [20], [29]. Together with the physical isolation action, the overall required start-up time was around 23 ms and the overall turn-off action was within 16 ms. The slight difference in the switching transient time, it comes from the charging and discharging characteristic of R_A. In the turn-on period, the energy comes from an auxiliary power, thus, the maximum supplying power is limited and it causes a longer time in charging. In the turn-on period, the energy comes from an auxiliary power, thus, the coil power is released through a freewheeling diode and a compensation resistor, thus, a fast discharging time is resultant.

In Fig. 12 (a), it shows the switching pattern that relates to the physical setting process, where R_2 and R_A are synchronized in action. During this processing period, the system did not have any power flow and operated at ZCS. It either worked to establish a system connection path at t_1 before the current flow began or produce the physical isolation at t_8 after the current return path was disconnected. In Fig. 12 (b), it shows the switching pattern that relates to the electrical operation process. S_A was only active during the switching transient at the dc breaker circuit. It provided an auxiliary path for the current conduction during the transient period. R_1 was only switched when S_A was active. Thus, it always operated with a parallel auxiliary path during the on-off action. A smoothly current transient waveform was observed in waveform and no electrical arc was visually observed from the experimental setup.

Under the purely resistive loading, the turn-on and turn-off switching performances of the semiconductor pair at the 150 Vdc system are shown in Fig. 13 (a) and (b), respectively. In both cases, the switching time was also maintained within 1 μs. It proved that the major restriction in the operation time of the hybrid circuit was mainly limited by the mechanical operation. If a faster system response is required, an ultra-fast mechanical ac relay can be considered in R_1 and the rest of the circuit does not affect. But there is a trade-off of cost and response time. Also, from Fig. 13, it demonstrates that the semiconductor pair is able to handle the transient responses in the dc breaker circuit properly and no over voltage scenario happens. Thus, a safe response was still able to be guaranteed.

For the designed platform, the maximum safety voltage capability is 380 Vdc. Under this condition, stable performance is able to guaranteed and is demonstrated in Fig. 14. In Fig. 14 (a), it shows a complete operating cycle of the proposed solution at 380 Vdc operating voltage, where the operation remains the same as in the 150 Vdc test case. Also, as shown in Fig. 14 (b), a fast semiconductor action is provided by S_A and no overvoltage scenario happens. Overall, the electrical operation time maintained within 8 ms and no electrical arc visually observed.

In Fig. 15, the platform serves with the same working condition as Fig. 14, where the only difference was the protection diode is eliminated in the test. Even a purely resistive load is connected, during the turn-off time period, the overvoltage situation was still easily triggered by the parasitic inductance and caused electrical stress to the semiconductors. Thus, it was important to have the protection diode in the design.

In order to verify the reliability and the bidirectional capability of the platform, a group of performance test has been done and is shown in Fig. 16 and Fig. 17, respectively. In Fig. 16, repeated interrupts are performed on the designed system. The test sequence is given with 200 ms per cycle at 150 Vdc and 15 A. Two sets of circuit prototypes were tested. Both of them were capable of running cycles above 100 thousand times, which was much higher than the traditional

mechanical solution shown in TABLE III. Thus, the high durability performance of the proposed solution is experimentally verified. In Fig. 17, a reverse conduction situation is demonstrated, in which the current direction is opposite to the test result in Fig. 12. Under the same circuit settings, it shows the same performance in both current directions. Thus, it proofed that the system was able to achieve stable performance in bidirectional current flow.

Apart from the normal shutdown operation, the system also performed stable under fault scenarios. In Fig. 18, it demonstrates the system performance at an over current scenario. In the evaluation, an inductive load was applied, which was formed by a 20 mH grid inductor and a 12.5 Ω electronic load. To perform the over current assessment, load transient was applied to result in an over-specified current to appear and the system would trigger when the current exceeded the limit of 15 A. In Fig. 18 (a), the output load was dropped from 12.5 Ω to 3 Ω and the system successfully disconnects both terminal connections at an overrating current, 48 A. Similarly, In Fig. 18 (b), the output load was dropped from 12.5 Ω to 1.67 Ω and the system successfully disconnects both terminals connection at an overrating current, 78 A. In both cases, the electrical switching time was maintained within 8 ms, low energy dissipation in all those relays, no electrical arcs were visually observed, and a correct semiconductor breaking waveform was observed. Meanwhile, the inductive energy was handled well by the protection diode after the circuit breaker was opened. All the performance was kept the same as the normal operation. Overall, a stable protection system was guaranteed.

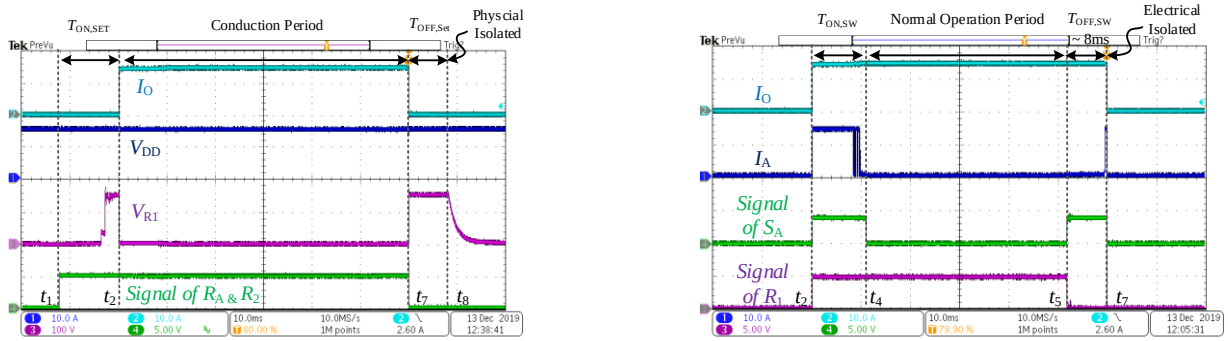

(a) (b)

Fig. 12 Experimental results under purely resistive loading that relates to (a) circuit isolation feature and (b) current conduction channel.

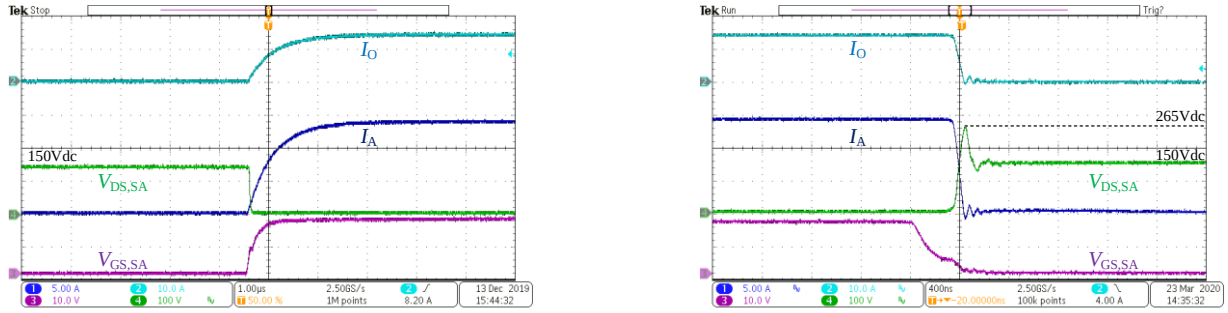

(a) (b)

Fig. 13 Experimental results of S_A under purely resistive loading at 150 Vdc 15A system, (a) turn-on transient at t_2 and (b) turn-off transient at t_7.

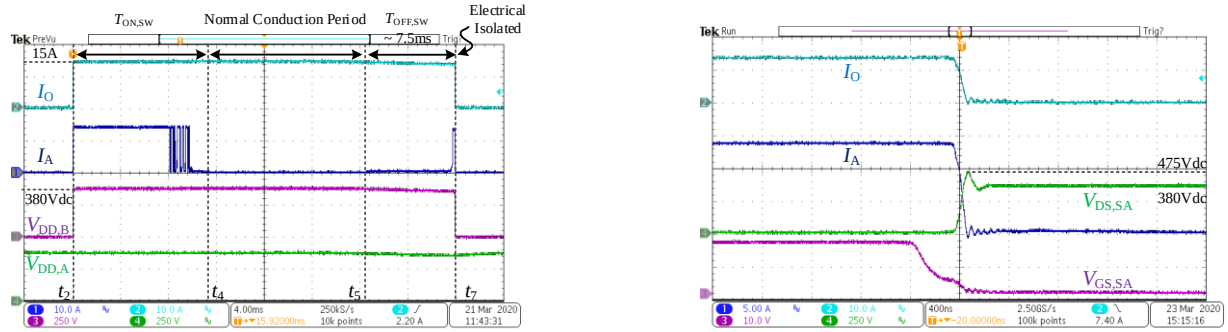

(a) (b)

Fig. 14 Experimental results under purely resistive load at 380 Vdc 15A system, (a) full cycle switching performance and (b) turn-off transient of S_A at t_7.

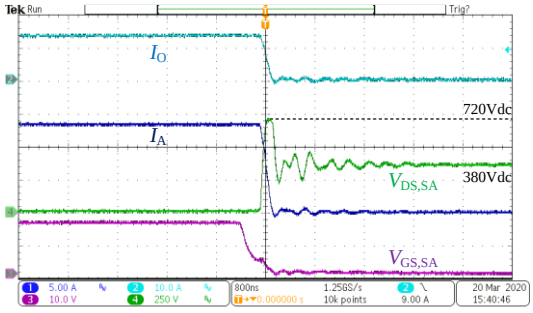

Fig. 15 Turn-off transient result of S_A in without diode protection situation.

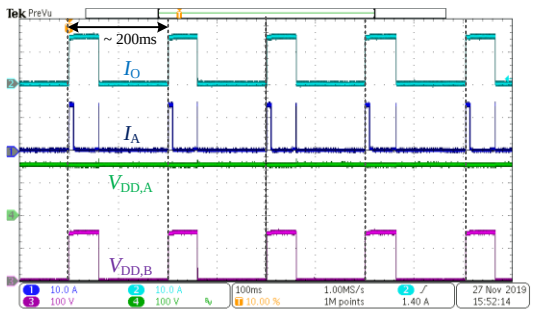

Fig. 16 Reliability testing sequence under pure resistive load.

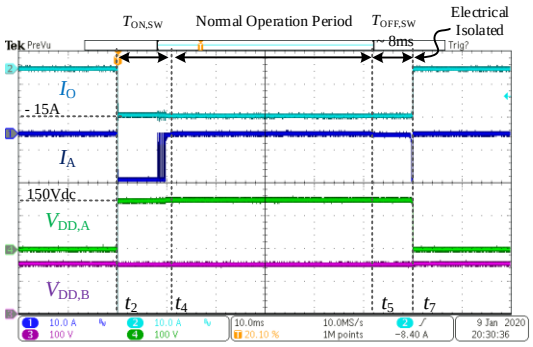

Fig. 17 Experimental result under reverse current flow.

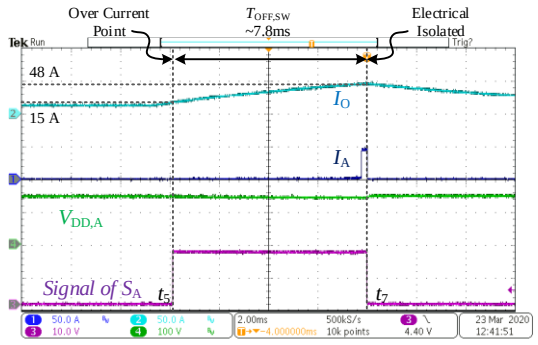

(a)

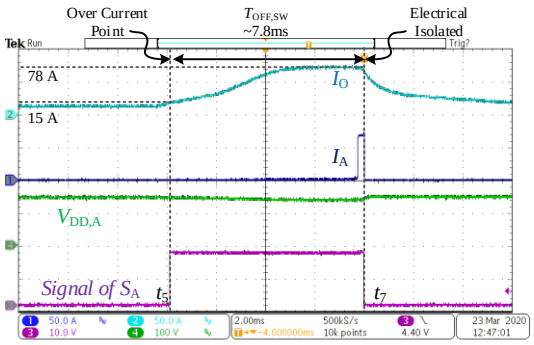

(b)

Fig. 18 Experimental results of overcurrent protection under inductive load, (a) breaking at 48A and (b) breaking at 78A.

V. Conclusion

The paper presented an alternative solution to the dc breaker design. In the concept, it makes use of both mechanical switches and semiconductor switches. Each of them deals with a key feature in the dc breaker. The mechanical switches focus on the normal conduction and the semiconductor switches handle the breaker transient. Therefore, the breaker design guarantees with bidirectional current flow, galvanic isolation, high reliability, and high efficiency for low voltage dc applications. The performance of the proposed concept was experimentally verified in a 250 V, 15A dc breaker setup, where the operation of both resistive and inductive loads have been tested. The results showed that the proposed solution achieved a fast response in switching action and was featured with high-reliability performance. All the demonstration results are shown with a good agreement is achieved between theoretical concepts and experimental results. The proposed dc hybrid breaker is promising for the applications of LV dc grid, PV array, and battery protection.

Reference

[1] Accetta and M. Pucci, "Energy Management System in DC Micro-Grids of Smart Ships: Main Gen-Set Fuel Consumption Minimization and Fault Compensation," *IEEE Trans. Ind. Appl.*, vol. 55, no. 3, pp. 3097-3113, May-Jun. 2019.

[2] Z. Jin, L. Meng, J. M. Guerrero, and R. Han, "Hierarchical Control Design for a Shipboard Power System With DC Distribution and Energy Storage Aboard Future More-Electric Ships," *IEEE Trans. Ind. Informat.*, vol. 14, no. 2, pp. 703-714, Feb. 2018.

[3] P. Sanjeev, N. P. Padhy, and P. Agarwal, "Peak Energy Management Using Renewable Integrated DC Microgrid," *IEEE Trans. Smart Grid*, vol. 9, no. 5, pp. 4906-4917, Sept. 2018.

[4] L. Roggia, L. Schuch, J. E. Baggio, C. Rech, and J. R. Pinheiro, "Integrated Full-Bridge-Forward DC–DC Converter for a Residential Microgrid Application," *IEEE Trans. Power Electron.*, vol. 28, no. 4, pp. 1728-1740, April 2013.

[5] A. Chub, D. Vinnikov, R. Kosenko, L. Liivik, and I. Galkin, "Bidirectional DC-DC Converter for Modular Residential Battery Energy Storage Systems," *IEEE Trans. Ind. Electron.*, vol. 67, no. 3, pp. 1944-1955, Mar. 2020.

[6] "Power generation system and inverter for feeding power into a three-phase grid", *US patent*, US8779630B2, 2009.

[7] "Method for checking a separation point of a photovoltaic inverter, and photovoltaic inverter", *US patent*, US9494659B2, 2012.

[8] "Detection of welded switch contacts in a line converter system", *US patent*, US20110298470A1, 2011.

[9] Y. Kishida, K. Koyama, H. Sasao, N. Maruyama, and H. Yamamoto, "Development of the high speed switch and its application," *Proc. IEEE Ind. Appl. Conf.*, Oct. 1998, pp. 2321–2328, vol. 3.

[10] J. Meyer and A. Rufer, "A DC hybrid circuit breaker with ultra-fast contact opening and integrated gate-commutated thyristors (IGCTs)," *IEEE Trans. Power Del.*, vol. 21, no. 2, pp. 646-651, Apr. 2006.

[11] "A hybrid circuit breaker", *European Patent*, EP2489053 (B1), 2009.

[12] C. Meyer, M. Kowal and R. W. De Doncker, "Circuit breaker concepts for future high-power DC-applications," *Industry Applications Conference*, vol. 2, pp. 860-866, Oct. 2005.

[13] J. Hafner and B. Jacobson, "Protective Hybrid HVdc Breakers - A Key Innovation for Reliable HVdc Grids," *CIGRE International Symposium*, Bologna, Sept. 2011.

[14] C. Peng, X. Song, A. Q. Huang, and I. Husain, "A Medium-Voltage Hybrid DC Circuit Breaker—Part II: Ultrafast Mechanical Switch," *Trans. Emerg. Sel. Topics Power Electron.*, vol. 5, no. 1, pp. 289-296, Mar. 2017.

[15] X. Song, C. Peng and A. Q. Huang, "A Medium-Voltage Hybrid DC Circuit Breaker, Part I: Solid-State Main Breaker Based on 15 kV SiC Emitter Turn-OFF Thyristor," *Trans. Emerg. Sel. Topics Power Electron.*, vol. 5, no. 1, pp. 278-288, Mar. 2017.

[16] C. Peng, A. Q. Huang, and X. Song, "Current commutation in a medium voltage hybrid DC circuit breaker using 15 kV vacuum switch and SiC devices," *Proc. IEEE APEC*, Mar. 2015, pp. 2244-2250.

[17] "HVDC hybrid circuit breaker with snubber circuit," *US Patent*, US8891209 (B2), 2011.

[18] "Hybrid dc circuit breaking device," *US Patent*, US20150022928 (A1), 2012.

[19] "High-voltage dc circuit breaker apparatus," *European Patent*, EP0108279 (B2), 1982.

[20] R. Lazzari and L. Piegari, "Design and Implementation of LVDC Hybrid Circuit Breaker," *IEEE Trans. Power Electron.*, vol. 34, no. 8, pp. 7369-7380, Aug. 2019.

[21] X. Pei, O. Cwikowski, A. C. Smith, and M. Barnes, "Design and Experimental Tests of a Superconducting Hybrid DC Circuit Breaker," in *IEEE Trans. on Appl. Supercond.*, vol. 28, no. 3, pp. 1-5, Apr. 2018.

[22] "Commutation type DC breaker", *US Patent*, US5452170A, 1992.

[23] D. Jovcic, "Series LC DC circuit breaker", *IET High Voltage*, vol, 4, iss. 2, pp. 130- 137, Jul. 2019.

[24] "Device and method for switching a direct current," *US Patent*, US20160300671 (A1), 2013.

[25] R. Ma *et al*., "Investigation on Arc Behavior During Arc Motion in Air DC Circuit Breaker," *IEEE Trans. on Plasma Sci.*, vol. 41, no. 9, pp. 2551-2560, Sept. 2013.

[26] Y. Kim and H. Kim, "Modeling for Series Arc of DC Circuit Breaker," *IEEE Trans. Ind. Appl.*, vol. 55, no. 2, pp. 1202-1207, Mar. - Apr. 2019.

[27] T. McDonald, M. Soldano, A. Murray, and T. Avram, "Power MOSFET Avalanche Design Guidelines," *International Rectifier Application Note*, AN-1005, Oct. 2004.

[28] J. S. Morton, "Circuit Breaker and Protection Requirements for DC Switchgear used in Rapid Transit Systems," *IEEE Trans. Ind. Appl.*, vol. IA-21, no. 5, pp. 1268-1273, Sept. 1985.

[29] D. Salomonsson, L. Soder, and A. Sannino, "Protection of Low-Voltage DC Microgrids," *IEEE Trans. Power Del.*, vol. 24, no. 3, pp. 1045-1053, Jul. 2009.

[30] S. Beheshtaein, R. Cuzner, M. Savaghebi, and J. M. Guerrero, "Review on microgrids protection," *IET Generation, Transmission & Distribution*, vol. 13, no. 6, pp. 743-759, Mar. 2019.